Journal of Engineering Research and Applied Science
Available at www.journaleras.com
Volume 12 (2), December 2023, pp 2401-2413
ISSN 2147-3471 © 2023

Investigation of the Natural and Artificial Radioactivity Levels in the Demirkaynak (Koza) Gold Mine Area (Gümüşhane, Türkiye) from the Perspectives of Environmental Geochemistry and Medical Geology

Alaaddin Vural[1,*], Ali Kaya[2]

[1,*]Ankara University, Faculty of Engineering, Geological Engineering, Ankara, Turkey
[2]Gümüşhane University, Faculty of Engineering and Natural Sciences, Physics Engineering Gümüşhane, Turkey

Accepted 11 December 2023

Abstract

The aim of this study is to investigate the levels of natural and artificial radioactivity in the soils of the Demirkaynak (Koza) mining site located in Gümüşhane (NE Türkiye), from the perspectives of environmental geochemistry and medical geology. For this purpose, ten soil samples were collected from selected points considering the lithological, general geological, and alteration characteristics of the site. The natural (^{226}Ra, ^{232}Th, and ^{40}K) and artificial (^{137}Cs) radioisotope activities of the collected soil samples were measured using appropriate analysis procedures with the Poptop Ortec Gamma-ray detector. The obtained activity values were utilized to calculate the radiation hazard indices of the sampling points, and an evaluation of the mining site soils was conducted within the context of medical geology and environmental geochemistry. The study revealed that the ^{226}Ra and ^{232}Th activities in the soils of the Demirkaynak (Koza) gold mining site did not exceed the weighted world average values (threshold values), while ^{40}K activities surpassed the weighted world average values (400 Bq/kg and/or 420 Bq/kg) in some sampling points. The elevated radioisotope activities in the area were found to be associated with intense development of hydrothermal alteration, indicating the effectiveness of alteration processes (potassic and sericitic alteration) in potassium (K) enrichments. The ^{137}Cs radioisotope activities in the area reached up to 3.3 Bq/kg, suggesting the presence of anthropogenic enrichment in the region. When considering the calculated radiation hazard indices for the site, it was observed that the absorbed dose rate values and annual effective dose rate values exceeded threshold values in some sampling points, indicating a significant level of radiation risk in the area.

Keywords: *Demirkaynak (Koza) Gold Mine, Natural radioactivity, Artificial radioactivity, Environmental geochemistry, Medical geology, Gümüşhane*

1. Introduction

Heavy metal contamination, along with natural and artificial radiation risks, stands out as prominent terminology when contemplating environmental issues. These concepts have become commonplace in discussions surrounding environmental concerns. Human-environment interaction, human-geological environment interaction started with the existence of humanity. However, in the past, the environmental problems caused by the products produced by people have not been brought to the agenda due to the small number of human population and the limited products they produce, as well as the lack of sufficient awareness about the environment [1]. The most striking environmental problems began with humanity's steps towards industrialization [2,3]. Awareness of environmental problems started in the 2nd half of the 20th century and continued to increase [2,4–6]. Previously, the environmental effects of heavy metals and trace elements were at the forefront [2,4,7–12]. The relationship between artificial radioactivity and the environment initially appeared to originate from nuclear testing, but the most significant awareness was heightened during the Second World War with the detonation of atomic bombs over two Japanese cities [13]. Subsequently, awareness regarding the environmental impact of natural radioactivity, as well as the effects of both natural and artificial radioactivity on the environment, particularly on human health, has increased. This has led to a proliferation of studies within this context. [14–16]. In fact, humans are consistently and inevitably exposed

[a]Corresponding author: alaaddinvural@hotmail.com

to natural radiation. However, the extent of this radiation exposure can vary, influenced by the geographical location of the human habitat and the geological/geochemical, as well as physicochemical characteristics of the environment. The primary source of radiation includes radioactive nuclei present in the structure of the Earth, along with cosmic rays originating from the solar system. These types of radiation sources are referred to as natural radiation. Additionally, radiation can also arise from technological products/tools produced by humans and/or as a result of human technological activities. Such radiation is defined as artificial radiation. In contemporary times, the most hazardous form of environmental radiation is artificial radiation stemming from nuclear reactor explosions or nuclear testing, which is of anthropogenic origin [14–17]. Despite this, recent studies indicate that approximately 80% of the total radiation exposure in recent years is attributed to natural radioisotope sources [18,19].

Prominent natural radiation sources include the radioisotopes uranium (U), thorium (Th), and potassium (K), along with their decay product nuclei (Figure 1). Living organisms are exposed to the radiations of these radioactive elements through the soil, where they carry out vital activities. Human activities, particularly agricultural practices and often habitation areas, predominantly occur on the relatively thin layer of the Earth's crust. In soil formation, the physicochemical, mineralogical, petrological, and geochemical characteristics of the parent rock contribute significantly, transferring these primary features to the soil. Thus, radioactive elements with long half-lives such as U, Th, and K transfer from the parent material to the soil, becoming the primary sources of natural radiation in the soil. Among these, ^{238}U, ^{235}U, ^{232}Th, and ^{40}K are the foremost radioisotopes [17,18,20]. These radioactive elements constitute the primary sources of external and internal radiation exposure for all matter, living organisms, and especially humans. The most significant source of internal radiation is the inhalation and/or ingestion of ^{222}Rn (radon) radioisotopes and their decay products, originating from the soil and rocks, reaching the atmospheric environment and eventually entering the human body through the direct and indirect pathways of the food chain. The decay of radium (Ra) from rocks, particularly abundant in the decay product of uranium found in granite rocks (Figure 1), facilitates the easy dispersion of the Rn element (Figure 1) [16,18–22].

External radiation, on the other hand, emanates from radioisotopes undergoing gamma decay in the uranium and thorium decay series (Figure 1) and naturally occurring potassium-40 (^{40}K), which is not a decay product of any radioactive heavy metal but forms naturally. Due to its long half-life and the abundance, especially in rocks near the Earth's surface, ^{40}K poses a radiation exposure risk comparable to ^{226}Ra. Prolonged exposure in environments with these radioisotopes increases the risk. Recent studies, in particular, confirm that granitic rocks exhibit high concentrations of such radionuclides (Figure 1) [6,22–27].

When considering anthropogenic radioisotopes, the most immediately recognizable and hazardous ones are ^{137}Cs, ^{131}I, ^{95}Zr, and ^{90}Sr, which emerge during nuclear power plant accidents or nuclear weapon testing. Among these isotopes, ^{137}Cs is the most dangerous and significant. For instance, it is estimated that during the first ten days following the Chernobyl nuclear power plant accident, approximately 70 PBq of ^{137}Cs and 330 PBq of ^{131}I were released into the atmosphere [28]. Due to the influence of winds prevailing during this period in various directions, radioactive materials were dispersed over a vast region, especially in Ukraine and the surrounding areas, including Europe in the northern hemisphere. The impact of ^{131}I was effective during the early stages of the accident and in close proximity due to the element's short half-life. However, the effects of the longer half-life radioisotopes, namely ^{134}Cs and ^{137}Cs, had the potential to spread to significant parts of the exposed body and persisted for many years [28–30]. The observation of artificial radionuclides originating from nuclear sources proves valuable in investigating the environmental impacts of nuclear power plants and nuclear tests. In this context, radioisotopes such as ^{137}Cs, with a half-life of 30.2 years, are particularly favored for their prolonged detectability.

Gümüşhane is situated within the Eastern Black Sea metallogenic belt, one of the foremost metallogenic zones in Türkiye. The region currently hosts numerous operational metallic ore deposits. Additionally, the area possesses significant underground resource potential in terms of industrial and energy raw materials. Consequently, there are numerous scientific studies in the region, addressing both general geology and mining geology objectives [31–37]. Taking into consideration the hydrothermal alteration and ore-forming processes experienced by the region, this study aims to investigate the natural and artificial radioisotope activities of the Demirkaynak (Koza) gold mining area, which is currently in operation and

represents the most significant ore deposit in the region. The research also seeks to explore the associated environmental impacts and potential risks on human health.

^{232}Th decay series			^{235}U decay series			^{238}U decay series		
Isotope	**Half-life**	**Decay type**	**Isotope**	**Half-life**	**Decay type**	**Isotope**	**Half-life**	**Decay type**
^{232}Th	1,4 x 10^{10}a	α	^{235}U	7,0 x 10^{8}a	a	^{238}U	4,5 x 10^{9}a	α
^{228}Ra	5,8 a	β	^{231}Th	26 h	b	^{234}Th	24 d	β
^{228}Ac	6,1 h	β	^{231}Pa	3,3 x 10^{4}a	a	^{234}Pa	6,8 h	β
^{228}Th	1,9 a	α	^{227}Ac	22 a	b	^{234}U	2,4 x 10^{5} a	α
^{224}Ra	3,7 d	α	^{227}Th	19 d	a	^{230}Th	7,3 x 10^{3}a	α
^{220}Rn	56 s	α	^{223}Ra	11,4 d	a	^{226}Ra	1,6 x 10^{3}a	α
^{216}Po	0,15 s	α	^{219}Rn	4,0 s	a	^{222}Rn	3,8 d	α
^{212}Pb	11 h	β	^{215}Po	1,8 ms	a	^{218}Po	3,1 m	α
^{212}Bi	61m	β	^{211}Pb	36,1 m	b	^{214}Pb	27 m	β
^{212}Po	0,30 µs	α	^{211}Bi	2,2 m	a	^{2I4}Bi	20 m	β
^{208}Pb	stable	——	^{207}Tl	4,8 m	b	^{214}Po	160µs	α
K, U and Th concentration in different environments (in ppm)			^{207}Pb	stable	——	^{210}Pb	22 a	b
			K	**U**	**Th**	^{210}Bi	5,0 d	b
CI Carbonaceous chondrites			**545**	**0,0074**	**0,029**	^{210}Po	138 d	a
Primitive mantle			**250**	**0,021**	**0,085**	^{206}Pb	Stable	——
Bulk silicate earth			**240**	**0,023**	**0,0795**			
Continental crust			**27500**	**2,5**	**10,5**	**Upper**		
			17500	**2,2**	**8,4**	**Middle (Archaean)**		
			8333	**0,05**	**0,42**	**Lower (Archaean)**		
			20000	**1,25**	**6**	**Lower and Middle (post Archaean)**		
Oceanic crust			**600**	**0,047**	**0,12**	**Normal Mid-Ocean Ridge Basalt (NMORB)**		
Ocean Island Basalt			**12000**	**1,02**	**4**	**(OIB)**		

Figure 1. Decay series of ^{232}Th, ^{235}U, and ^{238}U radioisotopes (from top to bottom) and concentrations of K, U, and Th elements in various environments in parts per million (ppm) [After 22]

1.1. General Geology of the Demirkaynak Mining Site and Its Surroundings

The Demirkaynak (Koza) gold mining area under investigation is situated in the southern zone of the Eastern Pontides, approximately 27 km northwest of the city center of Gümüşhane (Türkiye) (Figure 2). The study has been designed to cover an approximate area of 2.5 km². The oldest unit of the mining area is represented by the Middle-Late Carboniferous-aged Gümüşhane Pluton (Granodiorite) [31,35,38–43]. Overlying this unit in a discordant manner is the Early-Middle Jurassic-aged Zimonköy Formation, characterized by volcanic and sedimentary features [44]. The Zimonköy Formation is overlying the Berdiga Formation, which consists of Late Jurassic to Early Cretaceous limestones [45]. The Late Cretaceous-aged Kermutdere Formation unconformably overlies these units and is predominantly composed of sedimentary rocks [46,47], and around Torul, they are intersected by Late Cretaceous-aged plutons. [48]. The Alibaba Formation, comprising sedimentary interbedded volcanic rocks, unconformably overlies the Kermutdere Formation and is of Eocene age [32,33,46,49,50]. These units have been intruded by coeval calc-alkaline granitic plutons in various regions [2,5,34,51–55]. In the field, the youngest units are represented by Quaternary-aged alluvium and travertines [56,57].

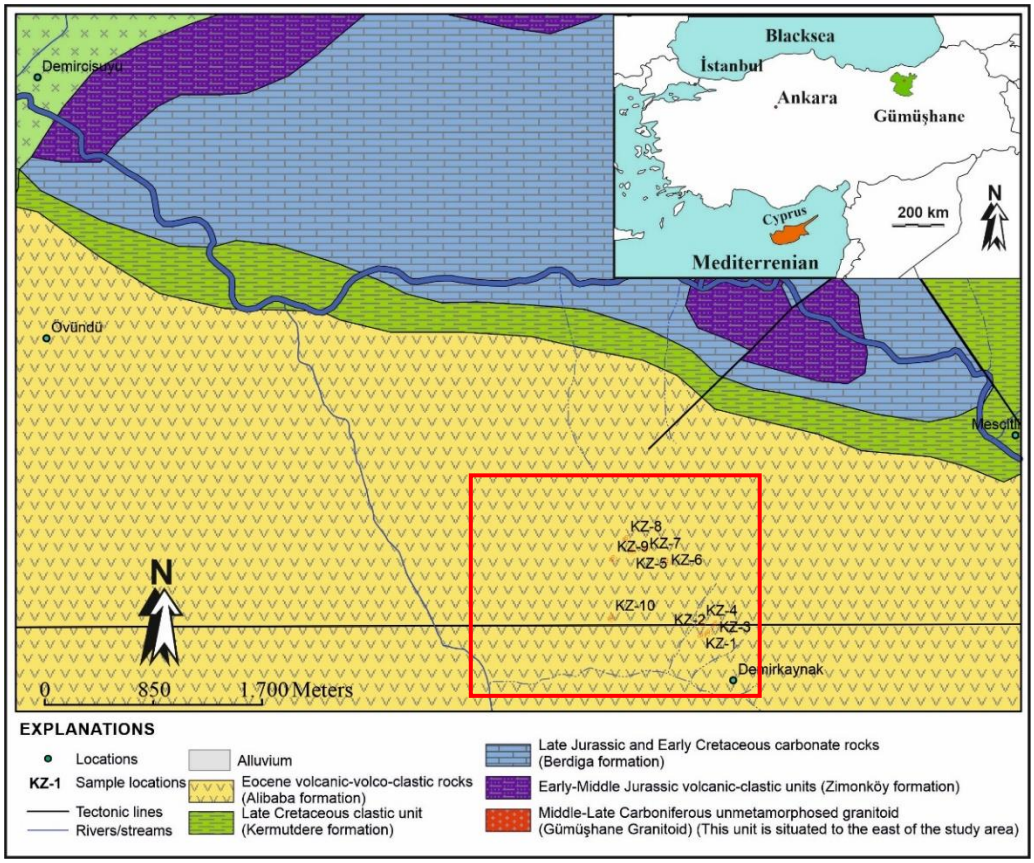

Figure 2. Location and general geological map of the Demirkaynak gold mine site (Gümüşhane, NE Türkiye) and its near vicinity (after [39,58])

2. Material and Methods

2.1. Sample Collection, Sample Preparation Processes

In order to determine the natural and artificial radioisotope activities of the mining site, 10 samples were collected from the Demirkaynak mining area. Samples were taken from points outside agricultural areas, cleared of organic matter around the sampling point, and collected from depths of 0-15 cm from the B level of the soil section. The sample collections from the mining site were conducted in September 2015. Sampling points were determined considering the ore formation and alteration characteristics and patterns of the site. Radioactive sampling procedures were followed during the sample collections. Macellan Explorist 710 handheld GPS was used for determining the coordinates of the sampling points, and the UTM WGS 1984 coordinate system was preferred. The samples were left at room temperature for an average of 10 days to remove their natural moisture. After passing through 2 mm Teflon sieves, the dried samples were transferred to Marinelli counting containers with sealed lids to prevent external air from entering. The weight of each sample was measured and recorded, and the lids of each container were securely locked. The establishment of radioactive equilibrium with the daughter radionuclide ^{222}Rn, which has a half-life of 3.82 days, occurs in periods ranging from 5 to 7 times that duration [59]. Therefore, to achieve radioactive equilibrium with ^{238}U and ^{232}Th in the structures of the samples taken from the study area, the samples were kept in a suitable environment for one month, and subsequently, their measurements were conducted using a gamma spectrometer at the Central Laboratory of Gümüşhane University (Gümüşhane, Türkiye). In addition to direct measurement methods, empirical methods are also employed in the measurements of radioisotope activities [60,61].

2.2. Radioisotope Activity Measurements of the Soil Samples

While determining the gamma radioactivity levels of the samples, the positioning of the detector and the sample according to the most suitable counting geometry is crucial. Marinelli containers provide the best conditions for this purpose, which is why they were preferred in this study. In cases where low-level radioactivity measurements are required, semiconductor detectors and scintillation detectors are

preferred. This is because semiconductor detectors have excellent energy resolution, making it easy to distinguish peaks that are very close to each other. Therefore, they are widely used in spectrometric gamma radiation measurements. Solid-state detectors used in gamma measurements are primarily manufactured using germanium and silicon. In these detectors, incoming radiation interacts with the crystal, losing its energy. As a result of these interactions, high-energy electrons detached from the crystal atoms interact with other electrons, creating ion pairs, and subsequently stabilize within a very short period, approximately 10^{-12} seconds. The accumulated charge is then drifted along the crystal by an externally applied electric field, generating an electrical signal. The obtained signal is recorded through an interface. The amount of charge generated within the crystal and accumulated on the contact surfaces is independent of the type of radiation but is solely proportional to the absorbed energy. The energy required for the formation of an electron pair is around 3 eV for semiconductors, 30 eV for gas ionization chambers, and approximately 300 eV for scintillation detectors. Photons with energies between 1 keV and 60 keV are measured using Si(Li) detectors, while those with energies between 5 keV and 10 MeV are measured using Ge(Li) or pure Ge(HPGe) detectors. Lithium atoms within Si and Ge crystals are highly mobile at elevated temperatures. Therefore, all three detectors are operated at liquid nitrogen temperatures (77º K). For the radioactivity measurements of the soils in the Demirkaynak gold mining area, a Poptop Ortec detector was utilized. Prior to the measurements, the baseline (background) radiation value of the detection chamber was routinely measured, and the detection limits for activity concentrations were calculated. IBM SPSS v.25 and Microsoft 365 Office Excel programs were used for the statistical evaluation of the measurement results of the natural and artificial radioisotope activities in the soil samples.

2.3. Radiation Indices

The effects of radiation, both artificial and natural, on humans and the environment are evaluated by calculating different indices and parameters. The radiation risks of the soil in the Demirkaynak gold mining area were assessed using parameters such as the absorbed dose rate (D), annual effective dose rate (AEDR), radium equivalent activity (R_{aeq}), and radiation hazard indices, including external hazard index (H_{ex}) and internal hazard index (H_{in}).

2.3.1. Absorbed Dose Rate (D)

The radiation risk associated with natural radioactive nuclei in the soil is typically expressed in terms of the absorbed dose rate (D) (nanoGray per hour, nGy/h) or exposure rate, usually at a height of 1 meter above the surface. Generally, artificial radioisotopes such as ^{137}Cs and ^{90}Sr, as well as the decay series of ^{235}U, are considered negligible. Therefore, absorber dose rates related to Th, Ra, and K radioisotopes, which predominantly contribute to natural radioactivity, are calculated [21,29]. In the calculation of the absorbed dose rate, average specific activity coefficients (Bq/kg to nGy/h) of 0.462 for U (in terms of Ra), 0.604 for Th, and 0.0417 for K are used. In cases where ^{137}Cs is considered, the coefficient for ^{137}Cs is 0.1125 (Bq/kg to nGy/h) [18,62]. The calculation of the absorbed dose rate is performed as follows (Equation 1). If the effect of anthropogenic artificial radioisotopes is also taken into account, the calculation is then carried out according to Equation 2 [63].

$$D(nGy/h) = 0.462A_{226_{Ra}} + 0.604A_{232_{Th}} + 0.0417A_{40_K} \quad (1a)$$

$$D(nGy/h) = 0.462A_{226_{Ra}} + 0.604A_{232_{Th}} + 0.0417A_{40_K} + 0.112A_{137_{Cs}} \quad (1b)$$

The formulas represent D, which corresponds to the absorbed dose rate and has a unit of nanoGray/hour (nGy/h). In natural environmental radioactivity conditions, the annual effective dose is calculated by multiplying the absorbed dose value by the factor 0.69 Sv Gy^{-1}. In the formulas, $A_{226_{Ra}}$, $A_{232_{Th}}$, A_{40_K} and $A_{137_{Cs}}$ respectively represent the activity concentrations of ^{226}Ra, ^{232}Th, ^{40}K, and ^{137}Cs. Global averages for absorbed dose rates have been calculated as 51 nGy/h, based on the medians of world Ra, Th, and K activities [29].

2.3.2. Annual Effective Dose Rate (AEDR)

Annual Effective Dose Rate (AEDR) is one of the most commonly used parameters in the context of medical geology. It is calculated using the absorbed dose rate in the air, and it estimates the effective dose received by humans using relevant coefficients. This parameter is employed to assess potential biological effects associated with ionizing radiation exposure in humans and is used for radiation protection purposes. The annual effective dose rate originating from natural terrestrial radionuclides is sometimes referred to as either natural annual effective dose rate ($AEDR_{nat}$) or terrestrial annual effective dose rate ($AEDR_{ter}$), and it is calculated according to Equation 2 [62]:

$AEDR_{nat}=0.69*D*[(1-I_{in})+SF.I_{in}]*24*365.25*10^{-3}$ (2)

The formula incorporates I_{in} (0.8) representing the indoor exposure factor, SF as the shielding factor (0.2), and the coefficient 0.69 ($SvGy^{-1}$), which is the conversion factor from absorbed dose in air to the effective dose for adults.

2.3.3. Radiation Hazard Indices

The external radiation hazard index *(H_{ex})* among the radiation hazard indices was proposed by [64] and expresses the risk associated with external gamma radiation sources. The external radiation hazard index is considered an acceptable dose of 1 mSv/year for the public. In soil, Hex is calculated using equation 3 and the internal radiation hazard index (Hin) is calculated using Equation 4:

$$H_{ex}=\frac{A_{226_{Ra}}}{370}+\frac{A_{232_{Th}}}{259}+\frac{A_{40_K}}{4810} \quad (3)$$

$$H_{in}=\frac{A_{226_{Ra}}}{185}+\frac{A_{232_{Th}}}{259}+\frac{A_{40_K}}{4810} \quad (4)$$

In the formula, parameters $A_{226_{Ra}}, A_{232_{Th}}, and\ A_{40_K}$ represent the activity concentrations of ^{226}Ra, ^{232}Th, and ^{40}K in Bq/kg, respectively. If the external hazard index *(H_{ex})* is greater than 1, it indicates that the external dose to which individuals are exposed has exceeded the acceptable level. To avoid radiation hazards to the respiratory organs, the internal radiation hazard index *(H_{in})* should be less than one (<1).

The overall impact of all radioactive nuclei on potential radiation is also calculated as radium equivalent activity (Ra_{eq}) [65]. The radium equivalent activity (Ra_{eq}) of the soil is calculated according to Equation 5, assuming an activity concentration of 370 Bq/kg for ^{226}Ra, 259 Bq/kg for ^{232}Th, and 4810 Bq/kg for ^{40}K. The explanations for the parameters in the equation have been provided above.

$$Ra_{eq(ex)}\ (Bq/kg)=A_{226_{Ra}}+1.429A_{232_{Th}}+0.077A_{40_K} \quad (5)$$

3. Results and Discussions

3.1. Radioisotope/radio nucleus activity assessments

In this study, the natural radioactivities of ^{232}Th, ^{226}Ra and ^{40}K, as well as the artificial radioactivity of ^{137}Cs, were measured in the soils of the Demirkaynak (Koza) gold mining area, and the results are presented in Table 1.

Table 1. The activity values (expressed as value ± standard deviation) for the elements Th, Ra, K, and Cs in the soils of the Demirkaynak (Koza) gold mining area. (Values highlighted in bold in the table correspond to exceeding the world-weighted average for the respective radioisotope)

Sample numbers	**^{232}Th**	**^{226}Ra**	**^{40}K**	**^{137}Cs**
1	**43±1.43**	12.7±0.18	**975.24±2.83**	0
2	**33±1.42**	14.5±0.08	**547±1.43**	3.3±0.01
3	**30±1.38**	12±0.26	330.6±1.28	1.5±0.01
4	27±1.25	13.5±0.18	**587±2.19**	1.3±0.01
5	**30±1.36**	12±0.25	**534±2.16**	0
6	25±1.33	15.6±0.27	**524±1.85**	0
7	11±0.62	16.8±0.23	236±1.28	2.3±0.04
8	16±0.78	17.8±0.36	**741±3.24**	1.5±0.03
9	24±1.26	23.1±0.32	**892.8±3.43**	0
10	23±1.23	13.9±0.04	**447.2±2.45**	0
Minimum	11	12	236	0
Maximum	43	23.1	**975.24**	3.3
Mean	26.20	15.19	**581.48**	0.99
Geo. Mean	24.68	14.89	**537.76**	
Std. Dev.	8.42	3.22	220.12	1.12
[18]	45	32	420	-
[66]	30	35 (for U)	400	

* Arithmetic means calculated without taking into account standard errors

The determined ^{232}Th activities in the soils of the Demirkaynak (Koza) gold mining area range from 11±0,62 to 43±1,43 Bq/kg. The average ^{232}Th activity for the entire site was found to be 26,20±8,42 Bq/kg (Table 1). It was observed that, in terms of ^{232}Th, none of the locations within the mining area exceeded the world-weighted average. However, when comparing the ^{232}Th values with the average values reported by [66] (30 Bq/kg), it was observed that four sampling locations exceeded the global average. The ^{226}Ra activities within the mining area were determined to range from 12±0,26 to 23,1±0,32 Bq/kg, with an average value of 15,19±3,22 Bq/kg (Table 1). Upon comparison with world-weighted ^{226}Ra averages, it was observed that none of the sampled locations exceeded global averages. The ^{40}K values in the soils of the study area were determined to range from 236±1,28 Bq/kg to 975,24±2,83 Bq/kg, with an average value of 581.48±220.12 Bq/kg (Table 1). As evident from the standard deviation, the ^{40}K values in the area do not exhibit a uniform distribution, indicating heterogeneity. This heterogeneity is attributed to the hydrothermal alteration experienced by the site. The measured radioactivity values of the artificial isotope ^{137}Cs in the soils of the Demirkaynak (Koza) mining area reveal that, in four sampling locations, the values remained below the detection limit. In the remaining eight sampling locations, the ^{137}Cs values were determined to range from 1,3±0,01 to 3,3±0,01 Bq/kg. The average activity of ^{137}Cs in the sampling locations where values exceeded the detection limit was found to be 0,99±1,12 Bq/kg (Table 1, Figure 3). As the ^{137}Cs radioisotope arises from anthropogenic influences, soil activities of ^{137}Cs are generally expected to be close to zero (Bq/kg). However, in the soils of the Demirkaynak mining area, ^{137}Cs activities were measured to reach up to 3 Bq/kg in a total of 5 sampling locations. Therefore, the possibility of anthropogenic influence in the Demirkaynak mining area and its immediate vicinity should not be overlooked (Table 1, Figure 3). When considering the reasons behind the elevated ^{137}Cs radioisotope activity, nuclear power plant accidents and/or nuclear weapon tests come to the forefront. Given Türkiye's nuclear potential, research capabilities, and opportunities in this field, there is no factor that would contribute to the increase in ^{137}Cs activities in the region.

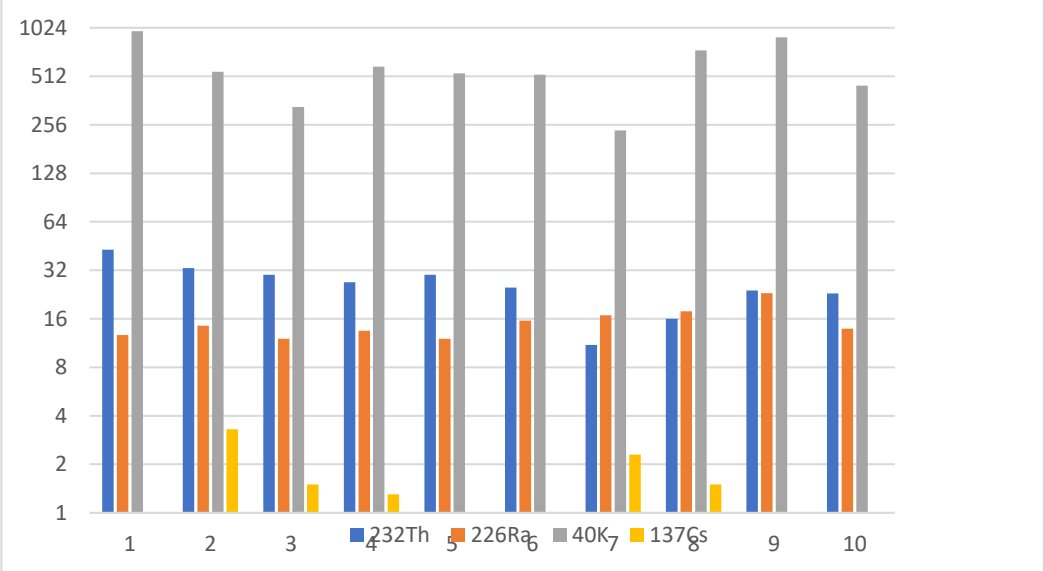

Figure 3. Graphs depicting the radioisotope/radionuclide activities of ^{232}Th, ^{226}Ra ^{40}K, and ^{137}Cs in the soils of the Demirkaynak (Koza) gold mining area are presented in the form of bar charts. The vertical axis is logarithmically scaled with a base of 2, and the unit is expressed in Bq/kg.

In considering the reasons for the elevated ^{137}Cs activity, regional-scale events come to mind. Foremost among these is the Chernobyl nuclear power plant accident in 1986, which stands as one of the largest nuclear accidents in history. Following the Chernobyl accident, a nuclear fallout cloud of considerable magnitude spread over a wide geography, affecting the northern hemisphere, especially Europe. Many countries in Europe, including Türkiye, were impacted by this radioactive fallout cloud. Chernobyl is located approximately 1400 km northwest of the Demirkaynak (Koza,

Gümüşhane, NE Türkiye) mining area, and considering the wind directions in the region, there is a potential risk of the region being affected by such an accident. For instance, in a study conducted on the soils of the Curonian Spit Forests in Lithuania after the Chernobyl accident, an activity value of 33.6 Bq/kg for ^{137}Cs was determined [30]. Another study in the Ignalina nuclear power plant region in Lithuania, conducted by [30], reported activation concentrations ranging from 4.8 to 8.4 Bq/kg. The obtained concentrations are compatible with the Chernobyl accident when considering the half-life of ^{137}Cs [27].

Another significant nuclear power plant accident is the Fukushima nuclear power plant accident in Japan in 2011. Numerous studies have been conducted to investigate the effects of the accident. These studies have revealed that, following the accident, various anthropogenic radioisotopes, including radio-cesium, were released into the atmosphere. In a study by [67], it was demonstrated that buildings, soils, various materials, and even humans in almost every part of the eastern region of Japan were affected by these radioactive fallout particles.

Following the Fukushima accident, a high concentration of ^{137}Cs reached the western part of North America on March 17, 2011, while a relatively lower concentration of the first air mass containing ^{137}Cs reached Europe on March 22, 2011, affecting the regions it passed through as precipitation [17]. Therefore, both the Chernobyl and Fukushima accidents have directly or indirectly impacted the northern hemisphere. While the most significant artificial radioisotope contaminations have been recorded in association with nuclear power plant accidents, contaminations related to nuclear weapons testing are also notably high. Records exist regarding the adverse effects of nuclear weapons testing in the United States. For instance, soils in areas such as Mount Rainier National Park, where nuclear weapons testing occurred within the boundaries of the state of Washington, and the Satsop Nuclear Power Plant region reported ^{137}Cs activities reaching up to 33.21 Bq/kg [30]. Nuclear activities and potential environmental impacts of nuclear accidents in countries where obtaining accurate information is challenging, such as China, Russia, and North Korea, remain insufficiently understood.

The assessment of soils from the Demirkaynak (Koza) gold mining area (Gümüşhane, NE Türkiye) in the context of human health/medical geology has been conducted using various radiation hazard indices. This evaluation is based on the natural radioisotope activities of ^{232}Th, ^{226}Ra, and ^{40}K, as well as the artificial isotope activities of ^{137}Cs. The obtained data are presented in Table 2.

Table 2. Radiation hazard indices for the Demirkaynak gold mining area. The red areas correspond to points of potential risk.

Sample numbers	**Hex (Limit 1)**	**Hin (limit 1)**	**Raeq (Limit 370)**	**D**	$AEDR_{nat}$
1	0.403	0.437	149.369	72.507	157.882
2	0.280	0.320	103.875	49.441	107.656
3	0.217	0.249	80.416	37.450	81.546
4	0.263	0.299	97.363	47.023	102.391
5	0.259	0.292	96.078	45.932	100.015
6	0.248	0.290	91.748	44.158	96.153
7	0.137	0.182	50.724	24.247	52.797
8	0.264	0.312	97.769	48.787	106.233
9	0.341	0.403	126.214	62.398	135.870
10	0.219	0.257	81.270	38.962	84.839
Minimun	0.137	0.182	50.724	24.247	52.797
Maximum	0.403	0.437	149.369	72.507	157.882
Mean	0.263	0.304	97.483	47.090	102.538
Geo. Mean	0.254	0.296	94.106	45.354	98.756
Std. Deviation	0.068	0.070	25.167	12.568	27.366
Limits	**1.00**	**1.00**	**370**	**51**	**111**

When the natural and artificial radioactivity values of the soils in the Demirkaynak (Koza) gold mining/ore deposit (Gümüşhane, NE Türkiye) area are collectively evaluated, it is generally observed that in areas with intense hydrothermal alteration and ore mineralization, the values of Th, Ra, and K tend to be around or exceed the weighted average values recommended by UNSCEAR (2000). The detection of ^{137}Cs activities in the soils of the area raises the possibility that the region may have been affected by the Chernobyl Nuclear Power Plant accident.

3.2. Radiation hazard indices

The external radiation index (H_{ex}) values for the soils of the Demirkaynak gold mining area were calculated to range from 0.137 to 0.403, with an average value of 0.263 (Geometric Mean: 0.254). It was determined that none of the sampling locations in the Demirkaynak mining area exceeded a value of 1 ($H_{ex}<1$) in terms of the external radiation hazard index (H_{ex}), indicating that the site does not pose a risk in terms of external radiation. The internal radiation index (H_{in}) for the area ranged from 0.182 to 0.437, with an average value of 0.304 (Geometric Mean: 0.296). Therefore, the soils in the area do not pose a risk in terms of the internal radiation index as well.

Considering the radium equivalent radiation (Ra_{eq}) values of the soils in the mining area, it was calculated that the Ra_{eq} values ranged from 50.72 to 149.37 Bq/kg, with an average Ra_{eq} value of 97,48 (Geometric Mean: 94,11) Bq/kg. When examining the Ra_{eq} values of the soils, rocks, or even materials exposed to radiation, attention is given to whether the calculated Ra_{eq} values are greater than 370 Bq/kg (the Ra_{eq} threshold value is 370 Bq/kg). It was determined that the calculated Ra_{eq} values for the soil samples in the Demirkaynak mining area did not exceed the value of 370 Bq/kg at any sampling location (Table 2).

For the Demirkaynak mining area, the absorbed dose rate (D) was calculated to range from 24.25 to 72.51 nGy/h, with an arithmetic mean of 47.09 (Geometric Mean: 45.35) nGy/h. It was observed that at only three sampling locations in the field, the global average absorbed dose rate (51 nGy/h) [18] was exceeded. Elevated values were associated with areas of intense alteration.

In this study conducted in the Demirkaynak area, it is envisaged that a more detailed investigation will be carried out, and regional-scale assessments will also be conducted. Therefore, annual effective dose rates for the site were calculated without considering the ^{137}Cs values. The annual effective dose rates for the soils of the site, calculated without taking into account the ^{137}Cs activities, were found to range from 52,80 to 157,88 μSv/y. The average annual effective dose rate for the site was determined to be 102.54 (Geometric Mean: 98.76) μSv/y. As detailed by Ali et al. [29], global effective dose rates are calculated based on the absorbed dose rate (51 nGy/h), with a median global annual effective dose rate estimated at 111 μSv/y. Considering the annual effective dose rates for the site, it was found that the threshold value was exceeded at only 2 sampling locations. A more detailed study of the sampling locations with elevated annual effective dose rates would be beneficial from a medical geology perspective.

In the region, several mining areas have been studied for the environmental effects of both natural and artificial radiation [16,25]. For instance, in a study conducted in the region characterized by hydrothermal alteration and metasomatic processes near Demirören village (Gümüşhane, Türkiye) [68], it was reported that both ^{40}K and ^{232}Th activities exceeded the recommended international weighted average values (400 Bq/kg and 30 Bq/kg, respectively). The researchers attributed the high K and Th activities detected in the region to hydrothermal/metasomatic processes. These processes contribute to the liberation of K, U, and Th elements, known to be abundant in minerals in the regional rocks, thereby causing an increase in the activities of these elements.

In a study conducted in the soils of the Eskiköy mining area, located to the north/northwest of the study area, [26] reported that U and Th radioisotope activities occasionally exceeded threshold values. The K activities in the mining area were found to be above the threshold at all sampling points. Therefore, the authors highlighted that the site exhibited noteworthy activity values for natural radioisotopes. For the same site, they indicated that the ^{137}Cs radioisotope activities were also at significant levels (3 Bq/kg), suggesting potential exposure to artificial radiation effects in the mining area.

[27] conducted an environmental/medical geological examination of natural and artificial radioisotope activities in the Karamustafa gold bearing Zn-Pb (±Cu) ore deposit located to the south/southwest of the Demirkaynak (Koza) mining area. They found that granitic rocks predominated across the general area of the mining site, and particularly in association with these lithological units, the activities of natural radioisotopes in the soils of the area were found to be

high. They suggested that in addition to lithological factors, hydrothermal processes contributing to mineralization would also contribute to the high activities of natural radioisotopes. They reported that the ^{137}Cs radioisotope activities in the mining area were high, likely due to anthropogenic influences, possibly from nuclear power plant accidents such as Chernobyl.

Studies by [69] and [25] were conducted in the ore-forming and alteration areas of Arzular-Dölek-Yitirmez (Gümüşhane, NE Türkiye), located to the east-northeast of Gümüşhane (Türkiye). In this study, it was reported that the natural radioisotope activities in the soils of the mining area exceeded threshold values for many sampling points concerning the relevant elements. They indicated that the concentrations of natural radioactivity in the area were related to the lithological characteristics of the region and the undergone hydrothermal alteration processes. They also mentioned that the artificial ^{137}Cs concentrations in the region occasionally exceeded 2 Bq/kg, indicating the presence of anthropogenic radiation traces in the region.

The elevated natural radioisotope activities in the study area, particularly with respect to the ^{40}K isotope, appear to be related to the general geological and lithological characteristics of the region and the hydrothermal alteration processes it has been exposed to, much like other mining areas in the region. Hydrothermal alteration processes play a significant role in the secondary geochemical dynamics of the geological environment. This is because primary hydrothermal fluids contain major cations such as Ca, Mg, K, Na, Mn, Ba, Fe, anions like C, Si, S, Cl, P, N, and elements including Pb, Cu, Zn, Ag, Au, U [70].. Gaseous types (H_2S, CO_2, SO_2, CH_4, N_2) and hydrocarbons are also commonly found in hydrothermal fluids. Potassic alteration is one of the widespread alteration types observed in hydrothermal processes. It is particularly common in epithermal ore formations like the Demirkaynak (Koza) gold deposit and porphyry ore systems developing in the deep sections of epithermal systems. The prevalent mineral characteristics of this hydrothermal alteration type include K-bearing feldspar and biotite. Another common hydrothermal alteration type is phyllic/sericitic alteration (quartz, sericite/illite, pyrite mineral assemblage). In this alteration type, there is also an enrichment of K in the geological environment. U and Th elements are large-sized and positively charged elements. Therefore, they cannot easily enter the composition of common magmatic rocks. As a result, they tend to concentrate in late-stage silica melts or in aqueous and gaseous fractions. Consequently, secondary minerals like rutile, apatite, titanite, monazite tend to contain these elements in their compositions. Thus, hydrothermal alteration processes can lead to the enrichment of natural radiogenic elements such as K, U (Ra), and Th in the geological environment. The widespread potassic and sericitic alteration in the epithermal-type gold ore occurence of the Demirkaynak (Koza) mining area has contributed to the notably high concentrations of K in the field. The ^{137}Cs radioisotope, as in other mining areas in the region, has also shown elevated levels in the Demirkaynak (Koza) mining area. This is believed to be influenced by the geographical location of the area, similar to other mining areas in the region, where radiation fallout possibly transported by active wind directions could have affected the region.

4. Conclusions

In this study, the natural and artificial radioisotope activities of the soil in the Demirkaynak gold mining area were assessed from the perspectives of environmental geochemistry and medical geology. The results of the study revealed relatively high natural radioisotope activities in the soil of the mining area, particularly exceeding the global average/threshold value in certain sections of the site, especially in terms of ^{40}K activities. It was concluded that the hydrothermal alteration processes experienced by the mining area and the lithological characteristics of the site significantly influenced the notable elevation of ^{40}K activities. The relatively high values of ^{137}Cs measured in the area (occasionally >3 Bq/kg) were attributed to the geographical location of the region, particularly associated with the Chernobyl Nuclear Power Plant accident in 1986, and this situation was considered as a potential anthropogenic pollution risk. The radioisotope activities of the site were evaluated using various radiation hazard indices. Taking into account the calculated radiation hazard indices, it was concluded that the Demirkaynak (Koza) gold mining area poses a risk in terms of absorbed dose rate and annual effective dose rates for some sampled locations.

Acknowledgments

This study was supported by the Scientific Research Coordination Unit of Gümüşhane University (Project No: 17.F5120.02.01). The authors extend their appreciation to GÜBAP for its generous support. The authors express their gratitude to Prof. Dr. Necati Çelik (Gümüşhane University) for his valuable support in determining the radioisotope activities.

References

[1] Vural A, Kaya S, Başaran N, Songören OT. Anadolu Madenciliğinde İlk Adımlar. Ankara, Türkiye: Maden Tetkik ve Arama Genel Müdürlüğü, MTA Kültür Serisi-3; 2009.

[2] Vural A. Trace/heavy metal accumulation in soil and in the shoots of acacia tree, Gümüşhane-Turkey. Bulletin of the Mineral Research and Exploration 2014; 148:85–106.

[3] Çiftçi A, Vural A, Ural MN. Analysis of Some Concepts Related to the Environment and Health with the N-Gram Method. Journal of International Health Sciences and Management 2021; 7:47–54.

[4] Vural A. Contamination assessment of heavy metals associated with an alteration area: Demirören Gumushane, NE Turkey. Journal of the Geological Society of India 2015; 86:215–222.

[5] Vural A. Relationship between the geological environment and element accumulation capacity of Helichrysum arenarium. Arabian Journal of Geosciences 2018; 11:258.

[6] Vural A, Albayrak M. Evaluation of Gördes zeolites in terms of mineralogical , geochemical and environmental effects. Journal of Engineering Research and Applied Science 2020; 9:1503–1520.

[7] Sungur A, Vural A, Gundogdu A, Soylak M. Effect of antimonite mineralization area on heavy metal contents and geochemical fractions of agricultural soils in Gümüşhane Province, Turkey. Catena 2020; 184:104255.

[8] Vural A. An evaluation of elemental enrichment in rocks: in the case of Kısacık and its neighborhood (Ayvacık, Çanakkale/Türkiye). Journal of Geography and Cartography 2023; 6:1–20.

[9] Vural A. On the elemental contents of aspen (Populus tremula L.) leaves grown in the mineralization area. Journal of Geography and Cartography 2023; 6:1–10.

[10] Vural A, Gündoğdu A, Saka F, Bulut VN. Geochemical investigation of the potability of surface water in Çit Stream and related creeks in Avliyana Basin (Gümüşhane , NE Türkiye). Turkish Journal of Analytical Chemistry 2022; 4:44–51.

[11] Vural A, Gündoğdu A, Saka F, Bulut VN, Soylak M. The Heavy Metals and Minor Elements Effects of Mineralization and Alteration Areas with Buried Ore Deposits Potential on the Surface Waters. Journal of Investigations on Engineering & Technology 2022; 5:21–33.

[12] Vural A, Gündoğdu A, Bulut VN, Alemdağ S, Saka F, Soylak M. Harşit Vadisinde (Gümüşhane), Bölgedeki (Terkedilmiş) Maden Sahalarından Kaynaklanan Ağır Metal/İz Element Kirliliğinin Araştırılması. Gümüşhane, Türkiye: 2020.

[13] Vural A, Ural MN, Çiftçi A. Yenilenebilir ve Nükleer Enerji Kaynaklarının Retrospektif Değerlendirilmesi. Journal of Investigations on Engineering & Technology 2022; 5:115–134.

[14] Higgy RH, Pimpl M. Natural and man-made radioactivity in soils and plants around the research reactor of Inshass. Applied Radiation and Isotopes 1998; 49:1709–1712.

[15] Miah FK, Roy S, Touhiduzzaman M, Alam B. Distribution of Radionuclides in soil samples in and around Dhaka city. Applied Radiation and Isotopes 1998; 49:133–137.

[16] Vural A. Investigation of the radiation risk to the inhabitants in the region close to the hydrothermal alteration site, Gümüşhane/Turkey. Journal of Engineering Research and Applied Science 2019; 8:1168–1176.

[17] Koo YH, Yang YS, Song KW. Radioactivity release from the Fukushima accident and its consequences: A review. Progress in Nuclear Energy 2014; 74:61–70.

[18] UNSCEAR. Sources, Effects and Risks of Ionizing Radiations. New York: 2000.

[19] UNSCEAR. United Nations Scientific Committee on the Effects of Atomic Radiation Report to the general assembly, with scientific annexes. 2008.

[20] Kaniu MI, Angeyo KH, Darby IG. Occurrence and multivariate exploratory analysis of the natural radioactivity anomaly in the south coastal region of Kenya. Radiation Physics and Chemistry 2018; 146:34–41.

[21] Krane SK. Introductory nuclear physics. New York: Wiley; 2008.

[22] Plant JA, Simpson PR, Smith B, Windley BF. Uranium ore deposits products of the radioactive Earth. Reviews in Mineralogy 1999; 38:255–319.

[23] Mason B, Moore C. Principles of geochemistry. Fourth. New York: Wiley; 1982.

[24] Rudnick R, Gao S. Composition of the Continental Crust. In: Holland H, Turekian K (eds.), Readings of Treatise on Geochemistry. 2nd ed. Londan, England: Elsevier; 2010.

[25] Vural A, Kaya A. Arzular-Yitirmez-Dölek (Gümüşhane) Maden/Alterasyon Sahalarındaki Doğal (226Ra, 232Th ve 40K) ve yapay (138Cs) Radyoaktivitelerine ait ilk değerlendirmeler. Euroasia Journal of Mathematics, Engineering, Natural & Medical Sciences 2021; 8:105–120.

[26] Vural A, Kaya A. Eskiköy Maden Sahasının (Gümüşhane, Türkiye) Doğal (^{226}Ra, ^{232}Th ve ^{40}K) ve yapay (^{138}Cs) Radyoaktivitelerine Bulgularına Ait İlk değerlendirmeler. Euroasia Journal of Mathematics, Engineering, Natural & Medical Sciences 2021; 8:133–150.

[27] Vural A, Kaya A. Assessment of Karamustafa Gold-Bearing Zn-Pb Mine (Gümüşhane, Türkiye) Area in Terms of Natural and Artificial Radioactivity. Göbeklitepe International Journal of Medical Sciences 2023.
[28] Bouville A. The Chernobyl Accident. Radiation Protection Dosimetry 1995; 60:287–293.
[29] Ali M, Wasim M, Iqbal S, Arif M, Saif F. Determination of the risk associated with the natural and anthropogenic radionuclides from the soil of Skardu in Central Karakoram. Radiation Protection Dosimetry 2013; 156:213–222.
[30] Jasaitis D, Klima V, Pečiulienė M, Vasiliauskienė V, Konstantinova M. Comparative Assessment of Radiation Background Due to Natural and Artificial Radionuclides in Soil in Specific Areas on the Territories of State of Washington (USA) and Lithuania. Water, Air, and Soil Pollution 2020; 231.
[31] Vural A, Erdoğan M. Eski Gümüşhane Kırkpavli Alterasyon Sahasında Toprak Jeokimyası. Gümüşhane Üniversitesi Fen Bilimleri Enstitüsü Dergisi 2014; 4:1–15.
[32] Vural A, Erşen F. Geology, mineralogy and geochemistry of manganese mineralization in Gumushane, Turkey. Journal of Engineering Research and Applied Science 2019; 8:1051–1059.
[33] Vural A, Akpınar İ, Kaygusuz A. Petrological characteristics of Cretaceous volcanic rocks of Demirören (Gümüşhane, NE Turkey) region. Journal of Engineering Research and Applied Science 2021; 10:1828–1842.
[34] Vural A, Kaygusuz A. Geochronology, petrogenesis and tectonic importance of Eocene I-type magmatism in the Eastern Pontides, NE Turkey. Arabian Journal of Geosciences 2021; 14:467.
[35] Vural A, Kaygusuz A. Petrology of the Paleozoic Plutons in Eastern Pontides: Artabel Pluton (Gümüşhane, NE Turkey). Journal of Engineering Research and Applied Science 2019; 8:1216–1228.
[36] Lermi A. Midi (Karamustafa/Gümüşhane, KD Türkiye) Zn-Pb Yatağının Jeolojik, Mineralojik, Jeokimyasal ve Kökensel İncelemesi. Karadeniz Teknik Üniversitesi, Trabzon, 2003.
[37] Yazıcı E., Dursun Ö, Güner S, Eroğlu Cİ, Selvi S, Deniz N. Gümüşhane-Bayburt-Artvin yörelerine ait epitermal altın aramaları. Ankara, Türkiye: 2010.
[38] Yılmaz Y. Petrology and structure of the Gümüşhane granite and surrounding rocks, NE Anatolia. 1972.
[39] Vural A. Evaluation of soil geochemistry data of Canca Area (Gümüşhane, Turkey) by means of Inverse Distance Weighting (IDW) and Kriging methods-preliminary findings. Bulletin of the Mineral Research and Exploration 2019; 158:195–216.
[40] Kaygusuz A, Arslan M, Siebel W, Sipahi F, Ilbeyli N. Geochronological evidence and tectonic significance of Carboniferous magmatism in the southwest Trabzon area, eastern Pontides, Turkey. International Geology Review 2012; 54:1776–1800.
[41] Kaygusuz A. Geochronological age relationships of Carboniferous Plutons in the Eastern Pontides (NE Turkey). Journal of Engineering Research and Applied Science 2020; 9:1299–1307.
[42] Topuz G, Altherr R, Siebel W, Schwarz WH, Zack T, Hasözbek A, Barth M, Satir M, Şen C. Carboniferous high-potassium I-type granitoid magmatism in the Eastern Pontides: The Gümüşhane pluton (NE Turkey). Lithos 2010; 116:92–110.
[43] Kaygusuz A, Arslan M, Sipahi F, Temizel İ. U-Pb zircon chronology and petrogenesis of Carboniferous plutons in the northern part of the Eastern Pontides, NE Turkey: Constraints for Paleozoic magmatism and geodynamic evolution. Gondwana Research 2016; 39:327–346.
[44] Eren M. Gümüşhane-Kale Arasının Jeolojisi ve Mikrofasiyes incelemesi. Karadeniz Teknik Üniversitesi, 1983.
[45] Pelin S. Alucra (Giresun) Güneydoğu Yöresinin Petrol Olanakları Bakımından Jeolojik İncelenmesi. Karadeniz Teknik Üniversitesi Yayınları 1977:87–103.
[46] Tokel S. Stratigraphical and volcanic history of Gümüşhane region. 1972.
[47] Saydam Eker C, Korkmaz S. Mineralogy and whole rock geochemistry of late Cretaceous sandstones from the eastern Pontides (NE Turkey). Neues Jahrbuch Fur Mineralogie, Abhandlungen 2011; 188:235–256.
[48] Kaygusuz A, Siebel W, Şen C, Satir M. Petrochemistry and petrology of I-type granitoids in an arc setting: The composite Torul pluton, Eastern Pontides, NE Turkey. International Journal of Earth Sciences 2008; 97:739–764.
[49] Arslan M, Temizel I, Abdioğlu E, Kolayli H, Yücel C, Boztuğ D, Şen C. 40Ar-39Ar dating, whole-rock and Sr-Nd-Pb isotope geochemistry of post-collisional Eocene volcanic rocks in the southern part of the Eastern Pontides (NE Turkey): Implications for magma evolution in extension-induced origin. Contributions to Mineralogy and Petrology 2013; 166:113–142.
[50] Aslan Z, Arslan M, Temizel İ, Kaygusuz A. K-Ar dating, whole-rock and Sr-Nd isotope geochemistry of calc-alkaline volcanic rocks around the Gümüşhane area: Implications for post-collisional volcanism in the Eastern Pontides, Northeast Turkey. Mineralogy and Petrology 2014; 108:245–267.
[51] Kaygusuz A, Yücel C, Arslan M, Temizel İ, Yi K, Jeong Y-J, Siebel W, Sipahi F. Eocene I-type

magmatism in the Eastern Pontides, NE Turkey: Insights into magma genesis and magma-tectonic evolution from whole-rock geochemistry, geochronology and isotope systematics. International Geology Review 2020.
[52] Vural A. K-Ar dating for determining the age of mineralization as alteration product: A case study of antimony mineralization vein type in granitic rocks of Gümüşhane area, Turkey. Acta Physica Polonica A 2017; 132:792–795.
[53] Vural A. Investigation of the relationship between rare earth elements, trace elements, and major oxides in soil geochemistry. Environmental Monitoring and Assessment 2020; 192:124.
[54] Kaygusuz A, Yücel C, Arslan M, Sipahi F, Temizel İ, Çakmak G, Güloğlu ZS. Petrography, mineral chemistry and crystallization conditions of Cenozoic plutonic rocks located to the north of Bayburt (Eastern Pontides, Turkey). Bulletin of the Mineral Research and Exploration 2018; 157:75–102.
[55] Karslı O, Chen B, Aydin F, Şen C. Geochemical and Sr-Nd-Pb isotopic compositions of the Eocene Dölek and Sariçiçek Plutons, Eastern Turkey: Implications for magma interaction in the genesis of high-K calc-alkaline granitoids in a post-collision extensional setting. Lithos 2007; 98:67–96.
[56] Vural A. Zenginleştirilmiş Jeoturizm Güzergahlarına Dair Farkındalık Oluşturulması : Eski Gümüşhane-Dörtkonak Güzergahı. Gümüşhane Üniversitesi Sosyal Bilimler Enstitüsü Elektronik Dergisi 2019; 10:250–274.
[57] Vural A, Külekçi G. Zenginleştirilmiş Jeoturizm Güzergahı:Gümüşhane-Bahçecik Köyü. Euroasia Journal of Mathematics, Engineering, Natural & Medical Sciences 2021; 8:1–23.
[58] Güven İH. Doğu Pontidlerin 1/100.000 Ölçekli Kompilasyonu. Ankara: MTA Genel Müdürlüğü; 1993.
[59] Chiozzi P, Pasquale V, Verdoya M. Radiometric survey for exploration of hydrothermal alteration in a volcanic area. Journal of Geochemical Exploration 2007; 93:13–20.
[60] Omeje M, Wagiran H, Ibrahim N, Lee SK, Sabris S. Comparison of Activity Concentration of 238U, 232Th and 40K in different Layers of Subsurface Structures in Dei-Dei and Kubwa, Abuja Northcentral Nigeria. Radiation Physics and Chemistry 2013; 91:70–80.
[61] Vural A. The Risk of Exposure to Natural Radiations Induced Hydrothermal Alteration Sites: Case of Canca Site (Gümüşhane, Türkiye). Göbeklitepe International Journal of Medical Sciences 2022; 5:14–22.
[62] Ali M, Iqbal S, Wasim M, Arif M, Saif F. Soil radioactivity levels and radiological risk assessment in the highlands of Hunza. Pakistan. Radiation Protection Dosimetry 2013; 153:390–399.
[63] Ribeiro FCA, Silva JIR, Lima ESA, do Amaral Sobrinho NMB, Perez D V., Lauria DC. Natural radioactivity in soils of the state of Rio de Janeiro (Brazil): Radiological characterization and relationships to geological formation, soil types and soil properties. Journal of Environmental Radioactivity 2018; 182:34–43.
[64] Krieger VR. Radioactivity of construction materials. Betonwerk Fertigteil Techn 1981; 47:468–473.
[65] Singh S, Rani A, Mahajan RM. ^{226}Ra, ^{232}Th and ^{40}K analysis in soil samples from some areas of Punjab and Himachal Pradesh, India using gamma ray spectrometry. Radiation Measurements 2005; 39:431–439.
[66] Chandrasankaran A, Ravisankar R, Senthilkumar G, Thillaivelavan K, Dhinakaran B, Vijayagopal P, Bramha SN, Venkatraman B. Spatial Distribution and Lifetime Cancer Risk due to Gamma Radioactivity in Yelagiri Hills, Tamilnadu, India. Egyptian Journal of Basic and Applied Science 2014; 1:38 – 48.
[67] Kato H, Onda Y, Gao X, Sanada Y, Saito K. Reconstruction of a Fukushima accident-derived radiocesium fallout map for environmental transfer studies. Journal of Environmental Radioactivity 2019; 210:105996.
[68] Vural A. Demiröreni/Gümüşhane-Türkiye Kuvars Porfiri Kayacı ve İlişkili Skarn-Metasomatizmanın Jeokimyasal Özellikleri. Euroasia Journal of Mathematics, Engineering, Natural and Medical Sciences 2020; 7:97–121.
[69] Kaya A, Çelik N, Vural A. Gümüşhane İlinde Maden Yataklarındaki/maden potansiyeli olan alterasyon sahalarındaki Topraktaki Doğal (^{226}Ra, ^{232}Th ve ^{40}K) ve Yapay (^{137}Cs) Radyoaktivite Konsantrasyonlarının Araştırılması. Gümüşhane, Türkiye: 2018.
[70] Pirajno F. Hydrothermal Processes and Mineral Systems. Avustralia: Springer Geological Survey of Western Australia; 2009.